Construction of Bio-functionalized ZnO Coatings on Titanium Implants with Both Self-Antibacterial and Osteoinductive Properties

Lei Tan, Xiangmei Liu, and Shuilin Wu

Abstract Bacterial infection and lack of osteoinductive ability are the major concerns of titanium-based bone implants. This chapter describes the construction of bio-functionalized ZnO coatings with both self-antibacterial and osteoinductive properties on titanium implants. To obtain ZnO-modified coatings with strong binding forces with substrates, two preparation methods are presented including atomic layer deposition and laser cladding techniques. Next, the antibacterial and osteoinductive properties of ZnO-based coatings are described including Ag/ZnO/hydroxyapatite-Ti, Ti-ZnO/polydopamine/arginine-glycine-aspartic acid-cysteine and poly(lactic-co-glycolic acid)/Ag/ZnO-Ti. We summarize the balancing strategies of reducing cytotoxicity of ZnO to bone cells and enhancing its toxicity towards bacteria.

Keywords Titanium implant · ZnO · Self-antibacterial · Osteoinductive · Atomic layer deposition · Laser cladding · Controlled release · Balancing

Introduction

It is well known that zinc ions possess both antibacterial and osteoinductive properties. The appropriate amount of zinc incorporated on the surface of implants can improve bone tissue integration and inhibit bone resorption [1, 2]. However, these biological functions are associated with release behavior because the excess release of zinc ions and related reactive oxygen species (ROS) can produce high cytotoxicity and thus inhibit the functions of improving bone formation [1]. On the contrary, high concentrations of zinc ion are helpful to its antibacterial effect. To address this

L. Tan · X. Liu
Ministry-of-Education Key Laboratory for the Green Preparation and Application of Functional Materials, Hubei Key Laboratory of Polymer Materials, School of Materials Science and Engineering, Hubei University, Wuhan, China

S. Wu (✉)
School of Materials Science and Engineering, Tianjin University, Tianjin, China
e-mail: shuilinwu@tju.edu.cn

B. Li et al. (eds.), *Racing for the Surface*,
https://doi.org/10.1007/978-3-030-34471-9_7

problem, the key point is to weaken the cytotoxicity of zinc ions towards bone cells and to enhance its toxicity towards bacteria to achieve both antibacterial and osteoinductive properties simultaneously.

As a promising zinc source, ZnO can be incorporated into and onto the coating of implants. From our previous investigations, we mainly chose two strategies to incorporate ZnO in the coating of Ti implants including atomic layer deposition (ALD) and laser cladding techniques [3, 4]. The ALD technique was first applied by Suntola et al. in 1970s [5]. Through two successive and cyclic sequentially self-limiting half-reactions, a controllable film can be prepared by a layer-by-layer mode on the surface of a substrate. Different from other methods such as vapor deposition, the thickness of the deposited film can be adjusted precisely through ALD at a monolayer level. Moreover, ALD can be operated under low deposition temperatures (even below ambient temperature), which makes it practicable to modify some thermal-sensitive substrates such as polymers [6]. As for the laser cladding method, it can increase the specific surface area, change the surface roughness, and increase the wettability of implants to influence the attachment and differentiation of bone cells [7]. Moreover, some ceramic powders such as hydroxyapatite (HA) can be fixed tightly on the surface of implants through laser melting [4, 8].

ZnO possesses good antibacterial ability through releasing Zn^{2+} and ROS or contact-killing. But the obvious cytotoxicity induced by a high concentration of Zn^{2+} and ROS can induce cell apoptosis and inhibit osteogenesis [1]. As for decreasing cytotoxicity of zinc ions to bone cells, we summarize three strategies according to our previous studies as follows: (1) chelating Zn^{2+} through coordination with a biocompatible coating; (2) reducing the produced ROS using an antioxidant; and (3) controlling the release behavior of Zn^{2+} and extending the release period [1, 4, 9, 10]. In order to balance the cytotoxicity and antibacterial activity of ZnO, the antibacterial performance of ZnO needs additional enhancement after the above treatments. Generally, Ag nanoparticles can be added to improve the antibacterial efficacy. Due to the synergistic antibacterial effect of Ag and Zn, only a small amount of Zn^{2+} and Ag nanoparticles is needed to kill bacteria efficiently [4, 9]. Besides, the additional antibacterial agents are not limited to Ag [10, 11]. Herein, we introduce two strategies of fabricating ZnO-decorated coatings on Ti implants and describe their antibacterial and osteoinductive behavior.

Fabrication and Characteristics of ZnO-Decorated Coatings on Ti Implants

The atomic layer deposition (ALD) technique is proven to be a promising strategy to fabricate a ZnO film on the surface of Ti implants. During deposition, diethyl zinc and H_2O are used as Zn and O precursors, respectively. Since the thickness of ZnO films is dependent on the cycle times, the content of ZnO on Ti implants can be well adjusted to control their biological functions. Based on this method, ZnO nanofilms could be deposited on the surface of carbon nanotubes/chitosan (CNT/CS) or titania nanotubes (TNTs) coatings [3]. Figure 1a shows the modified CNT/CS coating on

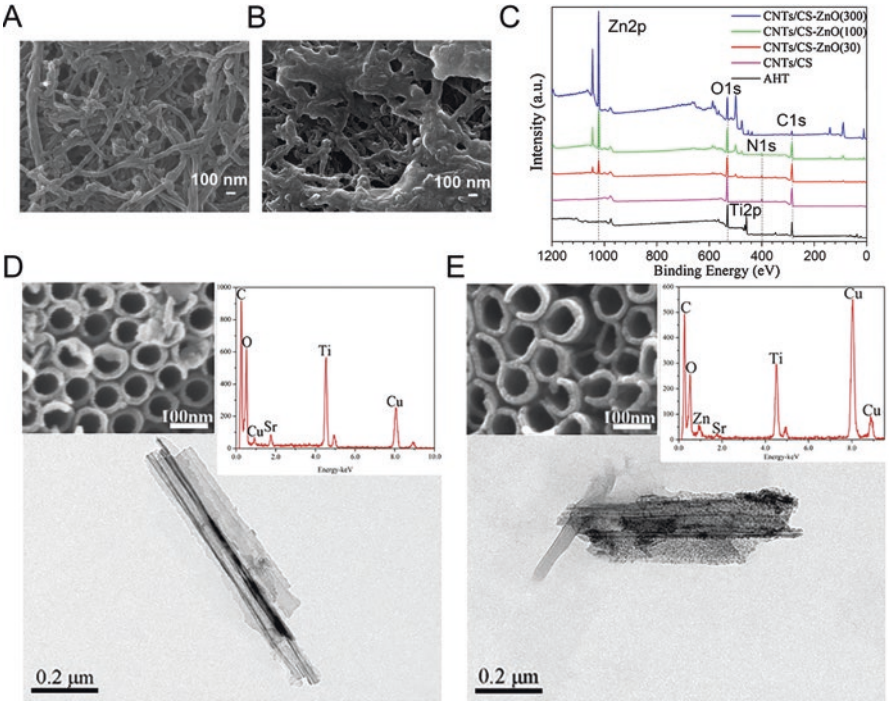

Fig. 1 FE-SEM images of (**A**) CNTs/CS and (**B**) CNTs/CS-ZnO (300 cycles). (**C**) XPS spectra of alkali-heat-treated Ti (AHT), CNTs/CS, CNTs/CS-ZnO (30 cycles), CNTs/CS-ZnO (100 cycles), and CNTs/CS-ZnO (300 cycles) [3]. (Copyright 2016. Adapted with permission from the Elsevier and Copyright Clearance Center.) FE-SEM (insert), EDS, and TEM images of (**D**) TNTs-Sr and (**E**) TNTs-Sr/ZnO [12]. (Copyright 2017. Adapted with permission from the Elsevier and Copyright Clearance Center)

the Ti implant via electrophoretic deposition. After depositing ZnO through the ALD technique, the dense nanoparticles distributed on CNT/CS were observed (Fig. 1b). From the X-ray photoelectron spectroscopy (XPS) results (Fig. 1c), the detected Zn element further proved the successful modification of ZnO nanofilms. The content of Zn increased with cycle times indicating that the content of ZnO could be regulated. Figure 1d shows the TNTs-Sr array on a Ti implant. It can be observed that the orifices of TNTs-Sr became rough after ZnO deposition (Fig. 1e). The signal of the Zn element was also detected by an energy dispersive spectrometer (EDS) [12]. Obviously, the ZnO nanofilms can be deposited uniformly on the surface of organic or inorganic coatings via the ALD technique.

Moreover, ZnO nanorods (NRs) arrays could grow from the ZnO seed layer (ZnOs) obtained by the ALD through hydrothermal method. Arginine-glycine-aspartic acid-cysteine (RGDC) peptide was covalently modified with Ti-ZnO/polydopamine (PDA) to improve osteogenesis (Fig. 2a). As shown in Fig. 2b, the size of ZnOs on Ti plate was around 20 nm. The hexagonal ZnO NRs with a 100 nm diameter were observed (Fig. 2c). Compared with ZnOs that is the

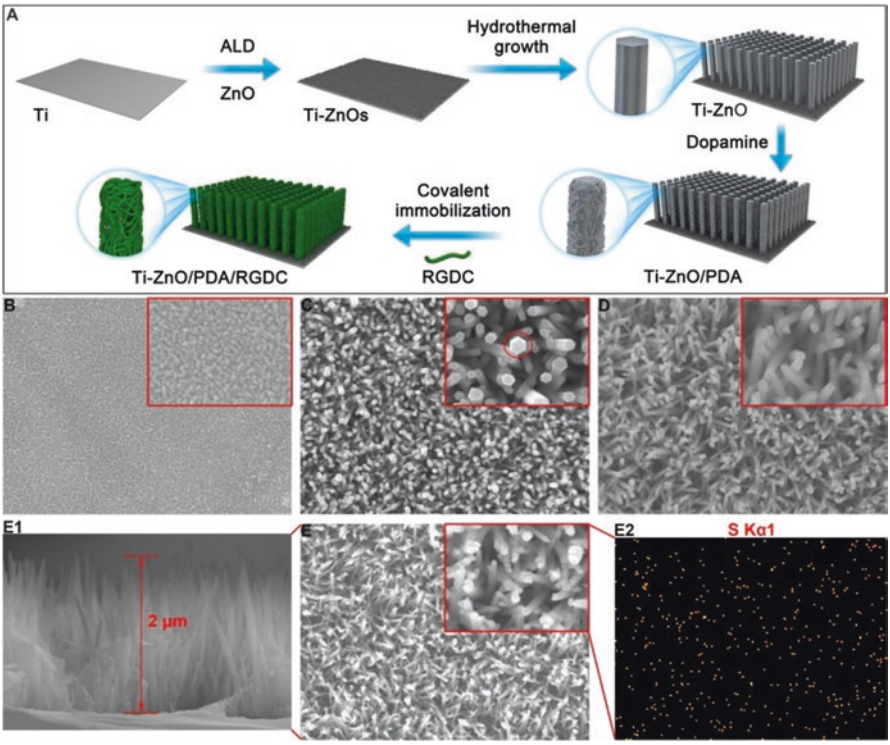

Fig. 2 (**A**) Schematic illustration of the fabrication process of the hybrid ZnO/PDA/RGDC NR arrays on Ti. FE-SEM images of (**B**) Ti-ZnOs (scale bars = 100 nm), (**C**) Ti-ZnO, (**D**) Ti-ZnO/PDA, and (**E**) Ti-ZnO/PDA/RGDC. (**E1**) Cross-sectional image of Ti-ZnO/PDA/RGDC. (**E2**) Elemental mapping of Ti-ZnO/PDA/RGDC, (scale bar = 100 nm (inset figure = 1 μm)) [1]. (Copyright 2017. Adapted with permission from the American Chemical Society)

ZnO seed layer (ZnOs) on Ti substrate obtained by ALD, ZnO NRs on Ti plate possessed a higher specific surface area and thus provided more active sites to improve the antibacterial performance and to increase the content of the modified RGDC. After the modification of PDA or RGDC, the surface of ZnO NRs became rougher (Fig. 2d, e). From the SEM image section (Fig. 2e1), the length of ZnO/PDA/RGDC NRs was approximately 2 μm. The detected S element proved the successful modification of RGDC (Fig. 2e2) [1].

In addition to the above methods of preparing ZnO films, our previous investigation shows that ZnO also can be incorporated with hydroxyapatite (HA) and Ag nanoparticles onto Ti6Al4V (Ti6) implants through laser cladding. The prefabricated Ag/HA and ZnO nanoparticles were first mixed and dispersed in deionized (DI) water. Then AgxZnOyHA dispersion was added to the surface of Ti6 and dried in a vacuum prior to laser cladding. The content of each component can be adjusted in the mixed powders for further antibacterial and osteoinductive investigation. The AgxZnOyHA modified Ti6 by laser cladding is shown in Fig. 3a. A regular texture

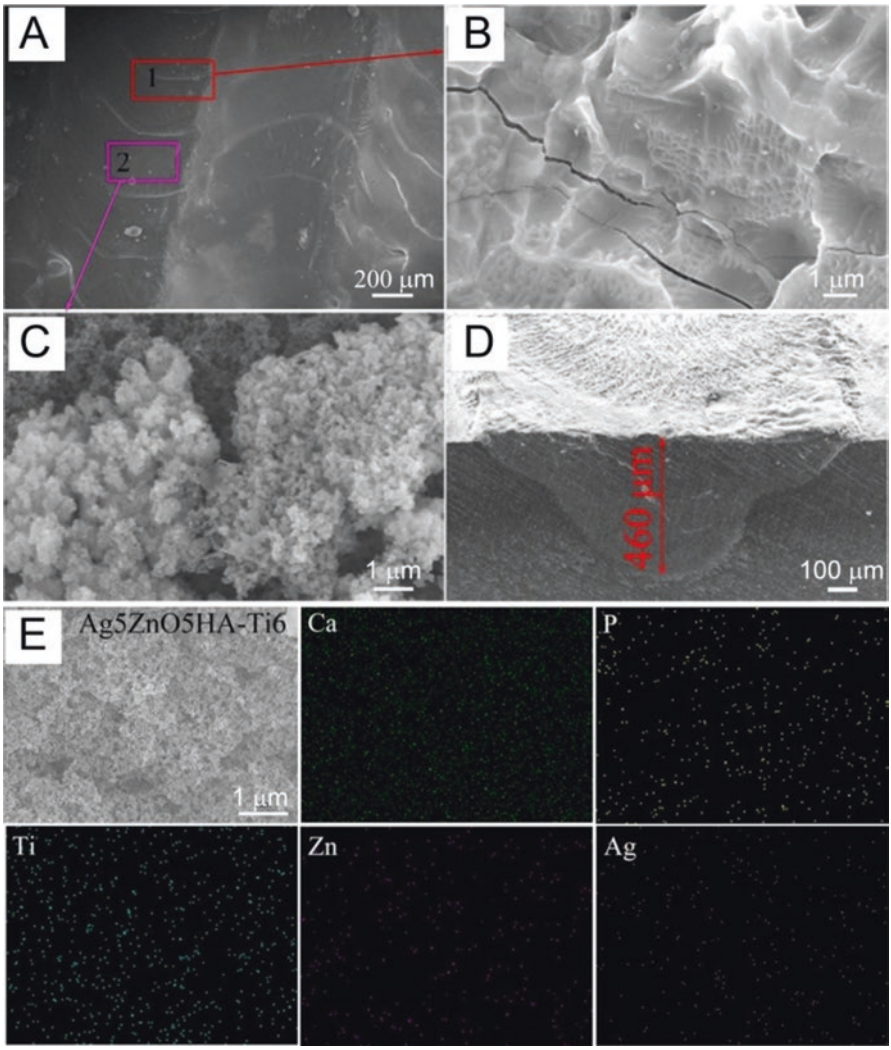

Fig. 3 (**A**) SEM image showing the surface morphology of the Ag5ZnO5HA-Ti6 (5:5:90, wt%) composite coating. (**B**) SEM image of bulging area (zone 1). (**C**) SEM image of the flat area (zone 2). (**D**) Cross-sectional SEM micrograph. (**E**) Elemental distribution by EDS [4]. (Copyright 2018. Adapted with permission from the American Chemical Society)

with parallel ridges was observed due to the back and forth movement of the laser spot which led to rapid melting and freezing of the composite on Ti6. The bulging areas of zone 1 (Fig. 3b) were attributed to the molten peaks while the flat areas of zone 2 (Fig. 3c) exhibited a loccular morphology, suggesting that the laser cladding can change the surface roughness of Ti6. From the section of the SEM image of AgxZnOyHA-Ti6 (Fig. 3d), the cladding with a 460 μm depth can be observed.

For the sample of the Ag5ZnO5HA-Ti6 sample, the EDS images showed that the elements of Ca, P, Ti, Zn, and Ag were uniformly distributed in the coating, indicating that these biofunctional elements were successfully introduced (Fig. 3e) [4].

Antibacterial Behavior Investigation

As we know, Zn^{2+} has antibacterial activity which is highly related to its content. However, high content or fast release can result in high cytotoxicity and cannot improve osteogenesis effectively. Benefiting from the laser melting of ZnO with coatings, the ZnO had a strong binding force with the coating. Therefore, the Zn^{2+} could be released slowly for 20 days (Fig. 4a). Whereas, the slowly release Zn^{2+} could not kill *Escherichia coli* (*E. coli*) or *Staphylococcus aureus* (*S. aureus*) efficiently. From Fig. 4b, c, the addition of Ag significantly increased antibacterial efficiency. On the contrary, the ZnO also could reduce the usage of Ag to lower its toxicity [4].

Due to the high specific surface area of ZnO NRs arrays on Ti (Ti-ZnO), the antibacterial performance of different modified ZnO NRs arrays were also investigated. Before that, the release behavior of Zn ions and ROS were first studied. As shown in Fig. 5a, a1, the release amount of Zn^{2+} in each group was similar, but the slight increased release of Zn^{2+} in Ti-ZnO/PDA-RGDC was due to that of the oxidation product of PDA which decreased the pH value (Fig. 5b, e). The decreased absorbance and faded color of PDA in the presence of Ti-ZnO demonstrated the antioxidant effect of PDA (Fig. 5c, d). Moreover, the electron spin resonance (ESR) results showed that Ti-ZnO generated an obvious more hydroxyl radical compared with Ti-ZnOs due to its higher specific surface area. However, the hydroxyl radical was decreased when PDA was introduced, which might weaken the antibacterial performance of Ti-ZnO (Fig. 5f). Besides, the released Zn^{2+} from Ti-ZnO/PDA could be chelated with the pyrocatechol of PDA (Fig. 5g, h), which thus might reduce the cytotoxicity [1].

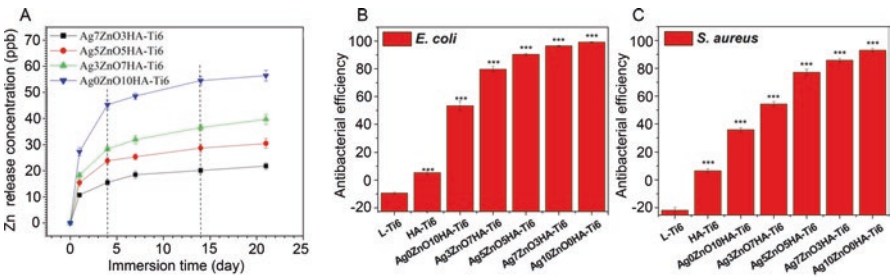

Fig. 4 (**A**) Release of Zn^{2+} from different ZnO nanoparticles (NPs). (**B**) Antibacterial efficiency of the samples compared to Ti6 for *E. coli*. (**C**) Antibacterial efficiency of the samples for *S. aureus*. The error bars indicate mean ± standard deviations: $***P < 0.001$ vs. L-Ti6 (*t* test) [4]. (Copyright 2018. Adapted with permission from the American Chemical Society)

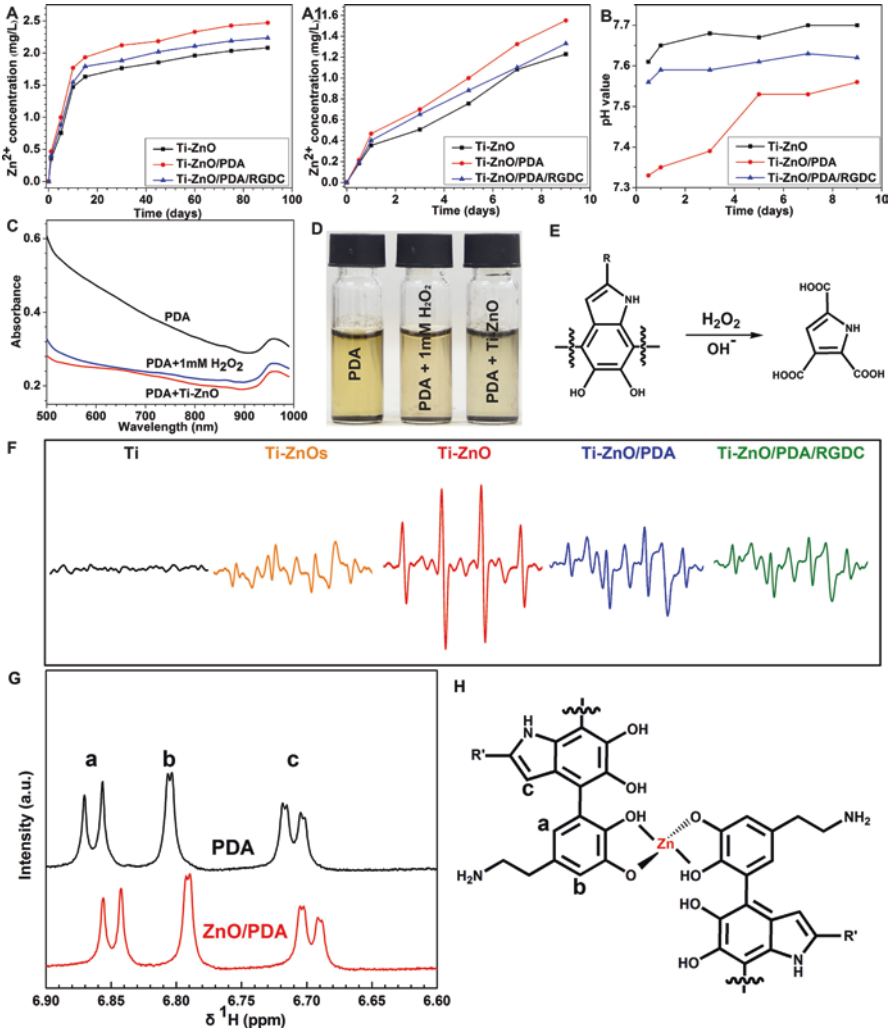

Fig. 5 (**A**) Cumulative zinc ion release curves of Ti-ZnO, Ti-ZnO/PDA, and Ti-ZnO/PDA/RGDC after immersion at 37 °C for 90 days. (**A1**) Short-term release; (**B**) pH values of the liquids corresponding to (**A1**). Degradation of PDA: (**C**) UV-vis absorption spectra, (**D**) corresponding photograph, (**E**) chemical degradation pathway of PDA by H_2O_2. (**F**) ESR spectra of Ti, Ti-ZnOs, Ti-ZnO, Ti-ZnO/PDA, and Ti-ZnO/PDA/RGDC. (**G**) HNMR spectra of PDA and PDA/ZnO [1]. (**H**) Structure of the Zn-PDA complex [1]. (Copyright 2017. Adapted with permission from the American Chemical Society)

The antibacterial behavior of samples was investigated by the spread plate method. As shown in Fig. 6a, the antibacterial rate of Ti-ZnO was much higher than Ti-ZnOs, indicating that ZnO NRs possessed better antibacterial ability. After modifying with PDA and RGDC, the antibacterial rates decreased but were still higher than 72%. From Fig. 6b, the antibacterial rate of Ti-ZnO/PDA-RGDC was much higher than Ti-ZnOs/PDA-RGDC [1].

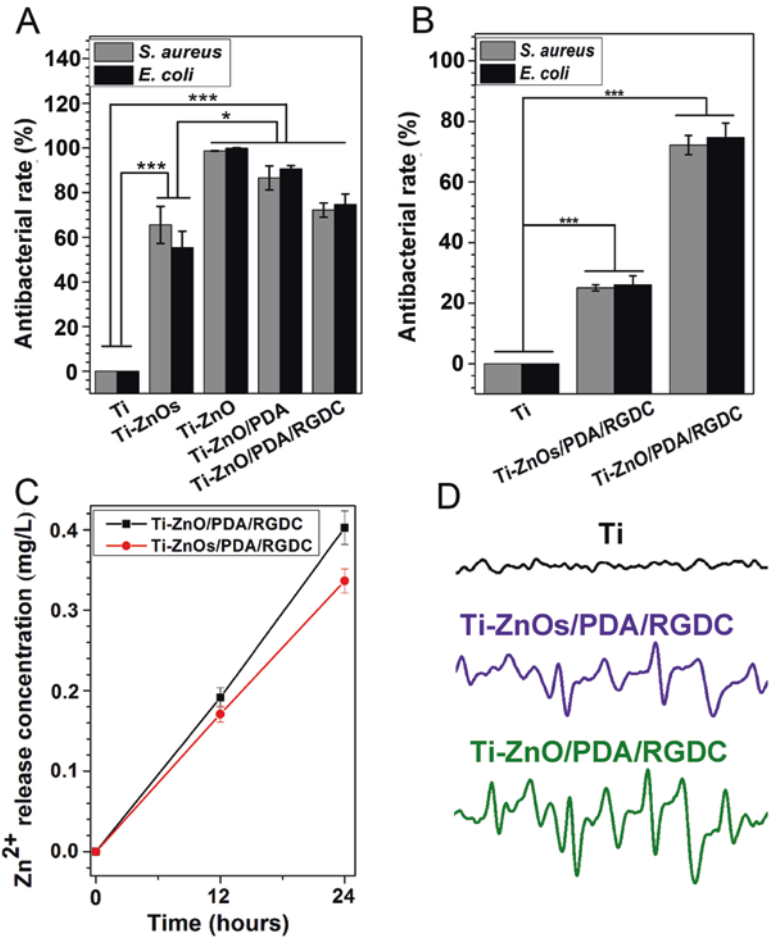

Fig. 6 (**A**, **B**) Antibacterial activity of the different samples. (**C**) Cumulative zinc ion release curves of Ti-ZnOs/PDA/RGDC and Ti-ZnO/PDA/RGDC after immersion at 37 °C for 1 day. (**D**) ESR spectra of Ti, Ti-ZnOs/PDA/RGDC and Ti-ZnO/PDA/RGDC. The error bars indicate mean ± standard deviations: $*P < 0.05$ and $***P < 0.001$ (*t* test) [1]. (Copyright 2017. Adapted with permission from the American Chemical Society)

Since the Ti-ZnOs/PDA-RGDC and Ti-ZnO/PDA-RGDC exhibited similar Zn^{2+} and hydroxyl radical release behavior, we speculated that the bacteria were physically punctured by Ti-ZnO/PDA/RGDC, which was proved by the TEM images of bacteria. As shown in Fig. 7, the bacteria treated by Ti-ZnO/PDA/RGDC showed obvious damages and were punctured by the needle-like NRs. Besides, the Zn^{2+} content was also higher than the Ti-ZnOs/PDA-RGDC group. These results showed that the physical puncture behavior and Zn^{2+} release of NRs had a synergistic antibacterial effect [1].

We also utilized poly(lactic-co-glycolic acid) (PLGA) to modify the ZnO NRs arrays because PLGA not only can control the release behavior of Zn^{2+} but can also

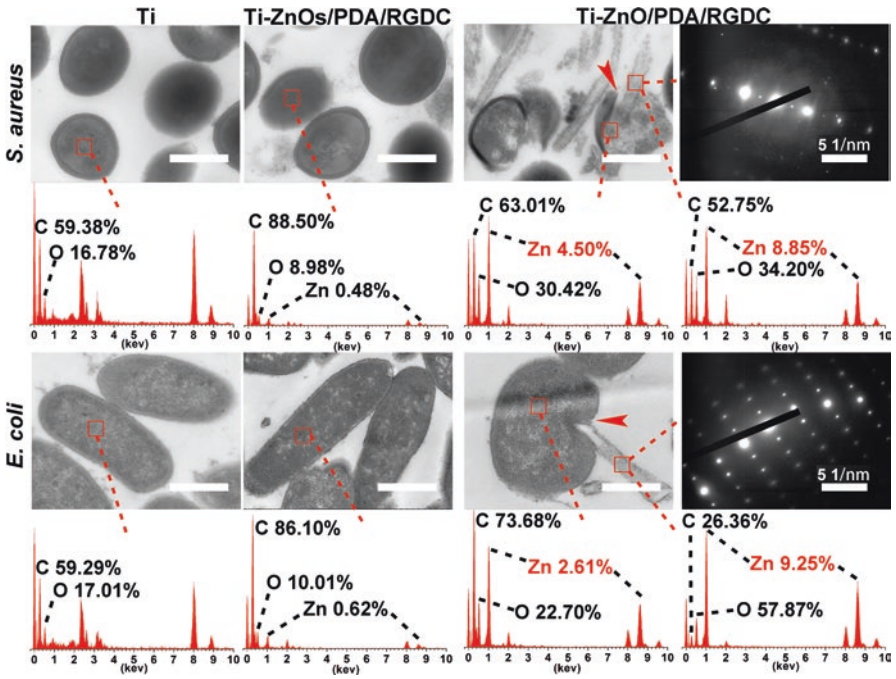

Fig. 7 TEM images of ultrathin section (about 70 nm) and the corresponding EDS of *S. aureus* and *E. coli* treated with Ti, Ti-ZnOs/PDA/RGDC, and Ti-ZnO/PDA/RGDC (scale bars = 500 nm) [1]. (Copyright 2017. Adapted with permission from the American Chemical Society)

reduce the cytotoxicity of ZnO NRs. The ZnO NRs surface showed a hydrophobic property due to its special nanostructure. The introduction of PLGA could increase the wettability of implant surfaces and thus be a benefit to the bone cell adhesion. However, the antibacterial ability of ZnO NRs was also weakened due to the coverage of PLGA. Our previous work showed that the antibacterial rate decreased from 94.1% to 70.3% against *S. aureus* after the modification of PLGA (PLGA/ZnO-Ti). Figure 8a, b shows that the surface of ZnO NRs was almost covered completely by a thick film after spinning PLGA. Unlike Ti-ZnOs/PDA-RGDC, the NRs structure was not maintained on the surface of PLGA/Ag/ZnO-Ti. The antibacterial performance of PLGA/ZnO-Ti is mainly attributed to the released ROS and Zn^{2+} but not the physical puncture effect. Similar to the abovementioned results, the introduction of Ag nanoparticles can further increase the antibacterial rate [9].

Osteoinductive Behavior Investigation

In addition to self-antibacterial property, the cytotoxicity and osteoinductive properties of Zn^{2+} cannot be ignored. The osteoinductive property of ZnO is attributed to the fact that the released Zn^{2+} can promote bone formation. However, high concentration

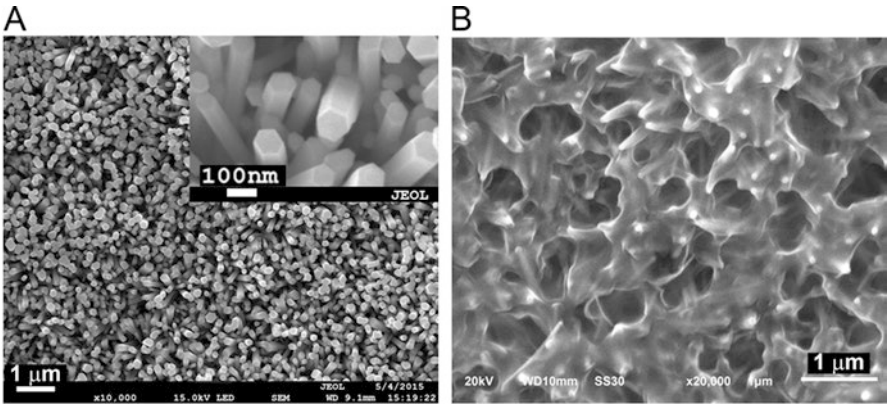

Fig. 8 (**A**) Morphological and microstructural characterization by the SEM image of ZnO nanorods. (**B**) SEM image of PLGA/3Ag/ZnO nanorods composite coating [9]. (Copyright 2017. Adapted with permission from the Elsevier and Copyright Clearance Center)

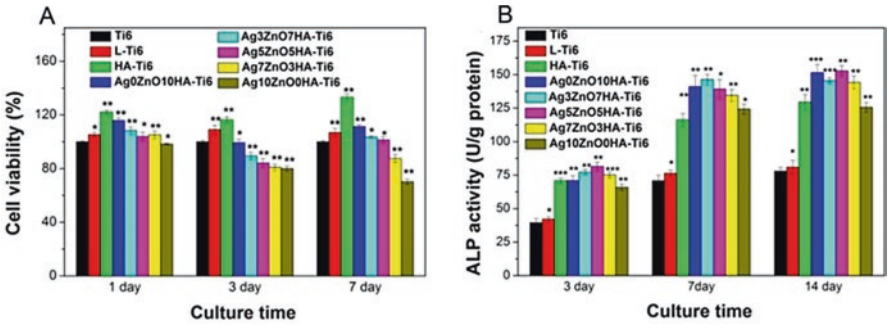

Fig. 9 (**A**) Cell viability assessed by MTT after culturing for 1, 3, and 7 days. (**B**) Cell osteogenesis evaluated by the ALP activity assay for 3, 7, and 14 days. The error bars indicate mean ± standard deviations: $*P < 0.05$, $**P < 0.05$, and $***P < 0.001$ vs. Ti6 (*t* test) [4]. (Copyright 2018. Adapted with permission from the American Chemical Society)

of Zn^{2+} can induce cytotoxicity and inhibit cell growth and bone tissue formation. We know that high concentration of Zn^{2+} possesses strong antibacterial ability. Therefore, how to use Zn^{2+} appropriately should be of concern. In the case of laser cladding method, the Zn^{2+} from Ag0ZnO10HA-Ti6 released quickly with cumulative concentration of 1.91 μg/L on day 4 because of some decorated ZnO on the surface, which was still lower than the safe concentration of 3 mg/L provided by the World Health Organization. Besides, quick release of Zn^{2+} is helpful to early infection prevention. After 4 days, the Zn^{2+} released slowly and steadily due to the strong fixation of ZnO in the composite coating (Fig. 4a). Benefiting from the release behavior of Zn^{2+}, the Ag0ZnO10HA-Ti6 exhibited high cell viability after 1, 3, or 7 days culture (Fig. 9a). It also showed that the alkaline phosphatase (ALP) activity of Ag0ZnO10HA-Ti6 was higher than the untreated Ti6, laser-treated Ti6,

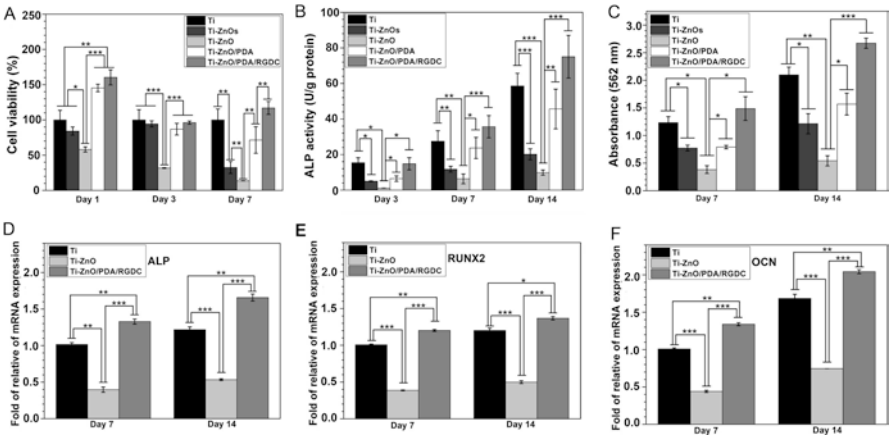

Fig. 10 (**A**) MTT assay of cell viabilities cultured in the medium with different samples after 1, 3, and 7 days. (**B**) Specific ALP activities of MC3T3-El osteoblasts cultured in the medium with different samples after 1, 3, and 7 days. (**C**) Quantitative measurement of the Alizarin Red staining after 7 and 14 days. Quantification of the osteoblast-related gene expressions of (**D**) ALP, (**E**) RUNX2, (**F**) OCN on Ti, Ti-ZnO, and Ti-ZnO/PDA/RGDC using normalization against a β-actin reference on the 7th and 14th day. The error bars indicate mean ± standard deviations: $*P < 0.05$, $**P < 0.05$, and $***P < 0.001$ (*t* test) [1]. (Copyright 2017. Adapted with permission from the American Chemical Society)

and HA-treated Ti6 on day 7 and day 14, suggesting that the osteogenesis ability of coating was obviously improved by the laser fixed ZnO. The appropriate addition of Ag nanoparticles not only did not influence the osteogenesis ability (Fig. 9b) but also showed efficient antibacterial performance [4].

As for ZnO NRs (Ti-ZnO), they exhibited high cytotoxicity after 1, 3, and 7 days towards MC3T3-El osteoblasts, which led to the lowest ALP expression. Although they could release Zn^{2+}, the osteoinductive behavior was mainly dominated by its high cytotoxicity. The cytotoxicity of ZnO was significantly decreased by the modification of PDA (Fig. 10a). We found that the ZnO NRs arrays could puncture bacteria but not osteoblasts, which could be explained by the fact that the size of osteoblasts is larger than bacteria and the bacteria were selectively punctured by ZnO NRs. After that, the ALP activity of Ti-ZnO/PDA increased compared to Ti-ZnO due to a decreased cytotoxicity and released Zn^{2+} from ZnO NRs (Fig. 10b). The modified RGDC further increased the ALP activity because it could promote cell attachment and improve osteogenic ability. The results of Alizarin Red staining and osteoblast-related gene expression further proved the great osteoinductive property of Ti-ZnO/PDA/RGDC (Fig. 10c–f) [1].

A bone implantation experiment in vivo was also conducted and we studied the osteoinductive property of Ti-ZnO/PDA/RGDC after 4 weeks. The results of micro-CT and Van Gieson's picro fuchsin staining showed that the newly formed bone tissues on the surface of implants obviously increased compared to Ti, suggesting that the decorated RGDC and released Zn^{2+} from ZnO NRs could accelerate osseointegration of the implants in vivo (Fig. 11) [1].

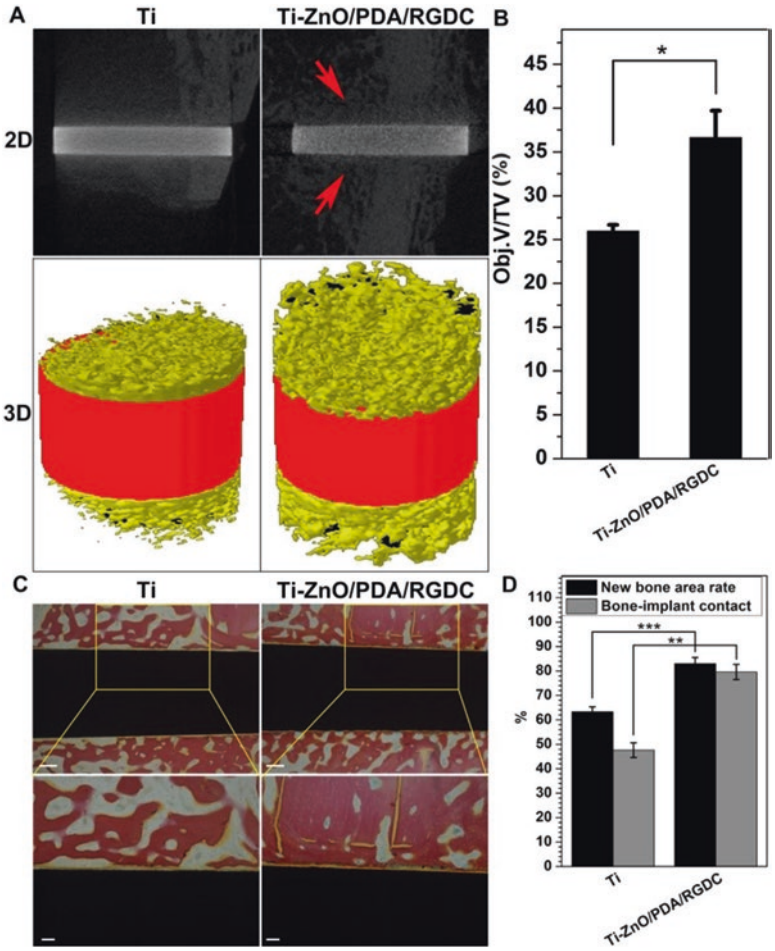

Fig. 11 (**A**) Micro-CT 2D and 3D images of new bone formation around the Ti and Ti-ZnO/PDA/RGDC implants in the rabbit femur 4 weeks after implantation. (**B**) Quantitative measurement of micro-CT 3D images of bone remodeling. (**C**) Histological characteristics at the bone-implant interfaces stained with Van Gieson's picro fuchsin (scale bars = 200 μm and 100 μm). (**D**) New bone area rate and bone-implant contact from the histomorphometric measurements. The error bars indicate mean ± standard deviations: $*P < 0.05$, $**P < 0.05$, and $***P < 0.001$ (t test) [1]. (Copyright 2017. Adapted with permission from the American Chemical Society)

Conclusion

This chapter focuses on the construction of bio-functionalized ZnO coatings with both self-antibacterial and osteoinductive properties on titanium implants. A laser cladding method fixed the ZnO tightly on the surface of substrates, which controlled the release of Zn^{2+} and thus showed great biocompatibility and improved the osteo-

inductive property. The additional antibacterial agent such as Ag nanoparticles enhanced the antibacterial performance of ZnO. The ALD technique provided a simple and mild method for preparing ZnO coatings with controlled thickness. Polymers such as PLGA and PDA reduced the cytotoxicity of ZnO NRs and the controlled release of Zn^{2+} can accelerate bone tissue integration. We believe that the successful balance of self-antibacterial and osteoinductive properties of ZnO can make it a promising coating for implants.

Future Directions

At present, the development of the bio-functionalized ZnO coatings still focuses on the modification of ZnO to control the release of Zn ions to improve the biocompatibility and osteoinductive ability. The antibacterial property of ZnO should be improved by additional antibacterial strategies through synergistic effect. All-in-one bio-functionalized ZnO coating is the future development direction. Moreover, our previous work reported that the bacteria on the surface of implants could be eliminated through near-infrared light [13]. Unlike the self-antibacterial behavior of endogenous antibacterial coatings, the bacteria can be killed rapidly and efficiently using exogenous irradiation. As for the photo-induced antibacterial application of ZnO, we prepared an antibacterial surface using red phosphorus/ZnO heterointerface to realize a light-activated rapid disinfection through the generation of ROS and heat (Fig. 12) [14]. However, the light source was solar light which cannot penetrate into

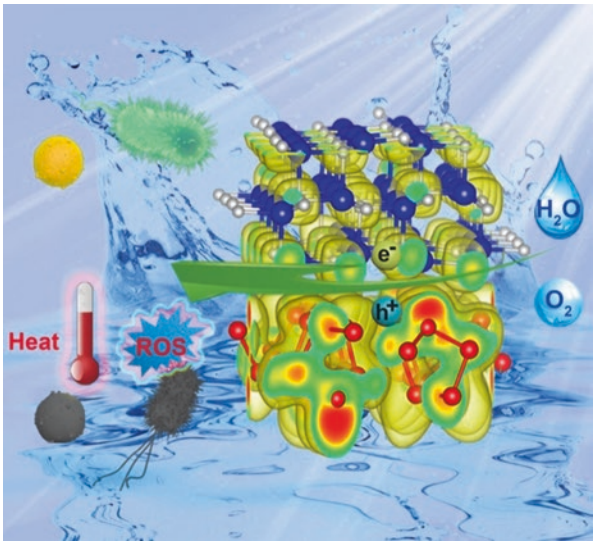

Fig. 12 Light-activated ultrafast bacterial inactivation due to the synergetic ROS and heat by RP/ZnO heterojunction [14]. (Copyright 2019. Adapted with permission from the John Wiley and Sons and Copyright Clearance Center)

the deep site of tissue. In the future, the key point is how to produce ROS or heat from ZnO-based coatings on implants using NIR light. So, the ZnO-based heterointerface or up-conversion nanoparticles can be incorporated into the coatings to realize NIR light induced disinfection on the surface of implant.

Acknowledgements This work was partially supported by the National Natural Science Foundation of China, Nos. 51801056, 51671081, 51871162, and 51422102, and the National Key Research and Development Program of China No. 2016YFC1100600 (subproject 2016YFC1100604), and the Natural Science Fund of Hubei Province, 2018CFA064. The authors also gratefully acknowledge the helpful comments and suggestions of the reviewers, which have improved the presentation.

References

1. Li J, Tan L, Liu X et al (2017) Balancing bacteria–osteoblast competition through selective physical puncture and biofunctionalization of ZnO/polydopamine/arginine-glycine-aspartic acid-cysteine nanorods. ACS Nano 11:11250–11263
2. Jung Kyu P, Yong-Jin K, Junseok Y et al (2010) The topographic effect of zinc oxide nanoflowers on osteoblast growth and osseointegration. Adv Mater 22:4857–4861
3. Zhu Y, Liu X, Yeung KWK, Chu PK, Wu S (2016) Biofunctionalization of carbon nanotubes/chitosan hybrids on Ti implants by atom layer deposited ZnO nanostructures. Appl Surf Sci 400:14–23
4. Zhang Y, Liu X, Li Z et al (2017) Nano Ag/ZnO incorporated hydroxyapatite composite coatings: highly effective infection prevention and excellent osteointegration. ACS Appl Mater Interfaces 10:1266–1277
5. Suntola T, Antson J (1977) Method for producing compound thin films: U.S. Patent 4,058,430 [P]. 11–15
6. George SM (2010) Atomic layer deposition: an overview. Chem Rev 110:111–131
7. Park JW, Kim Y, Park C et al (2009) Enhanced osteoblast response to an equal channel angular pressing-processed pure titanium substrate with microrough surface topography. Acta Biomater 5:3272–3280
8. Comesaña R, Quintero F, Lusquiños F et al (2010) Laser cladding of bioactive glass coatings. Acta Biomater 6:953–961
9. Xiang Y, Li J, Liu X et al (2017) Construction of poly(lactic-co-glycolic acid)/ZnO nanorods/Ag nanoparticles hybrid coating on Ti implants for enhanced antibacterial activity and biocompatibility. Mater Sci Eng C 79:629–637
10. Wang T, Liu X, Zhu Y et al (2017) Metal ion coordination polymer-capped pH-triggered drug release system on titania nanotubes for enhancing self-antibacterial capability of Ti implants. ACS Biomater Sci Eng 3:816–825
11. Li Y, Liu X, Tan L et al (2017) Construction of N-halamine labeled silica/zinc oxide hybrid nanoparticles for enhancing antibacterial ability of Ti implants. Mater Sci Eng C 76:50–58
12. Zhang K, Zhu Y, Liu X et al (2017) Sr/ZnO doped titania nanotube array: an effective surface system with excellent osteoinductivity and self-antibacterial activity. Mater Des 130:403–412
13. Tan L, Li J, Liu X et al (2018) Rapid biofilm eradication on bone implants using red phosphorus and near-infrared light. Adv Mater 30:1801808
14. Li J, Liu X, Tan L et al (2019) Light-activated rapid disinfection by accelerated charge transfer in red phosphorus/ZnO heterointerface. Small Methods 3:1900048